

## A SUBMILLIMETER AND RADIO SURVEY OF GAMMA-RAY BURST HOST GALAXIES: A GLIMPSE INTO THE FUTURE OF STAR FORMATION STUDIES

E. BERGER,<sup>1</sup> L. L. COWIE,<sup>2</sup> S. R. KULKARNI,<sup>1</sup> D. A. FRAIL,<sup>3</sup> H. AUSSEL,<sup>2</sup> AND A. J. BARGER<sup>2,4,5</sup>

Received 2002 October 29; accepted 2003 January 15

### ABSTRACT

We present the first comprehensive search for submillimeter and radio emission from the host galaxies of 20 well-localized gamma-ray bursts (GRBs). With the exception of a single source, all observations were undertaken months to years after the GRB explosions to ensure negligible contamination from the afterglows. We detect the host galaxy of GRB 000418 in both the submillimeter and radio, and the host galaxy of GRB 000210 in only the submillimeter. These observations, in conjunction with the previous detections of the host galaxies of GRB 980703 and GRB 010222, indicate that about 20% of GRB host galaxies are ultra-luminous ( $L > 10^{12} L_{\odot}$ ) and have star formation rates of about  $500 M_{\odot} \text{ yr}^{-1}$ . As an ensemble, the non-detected hosts have a star formation rate of about  $100 M_{\odot} \text{ yr}^{-1}$  ( $5 \sigma$ ) based on their radio emission. This, in conjunction with an average luminosity for the entire sample that is approximately 20% fainter than the local starburst galaxy Arp 220, indicates that GRB hosts probe a more representative population of star-forming galaxies than those uncovered in blank submillimeter and radio surveys. The detected and ensemble star formation rates exceed the values determined from various optical estimators by an order of magnitude, indicating significant dust obscuration. In the same vein, the ratio of bolometric dust luminosity to UV luminosity for the hosts detected in the submillimeter and radio bands ranges from about  $\sim 30$  to 500 and follows the known trend of increasing obscuration with increasing bolometric luminosity. We also show that the GRB host sample as a whole, and the submillimeter- and radio-detected hosts individually, have significantly bluer  $R-K$  colors as compared with galaxies selected in the submillimeter and radio in the same redshift range. This possibly indicates that the stellar populations in the GRB hosts are on average younger, supporting the massive stellar progenitor scenario for GRBs, but it is also possible that GRB hosts are on average less dusty. For the nondetected GRB hosts, the difference in  $R-K$  color may also be a manifestation of their more representative bolometric luminosities relative to the highly luminous submillimeter- and radio-selected galaxies. Beyond the specific results presented in this paper, the submillimeter and radio observations serve as an observational proof-of-concept in anticipation of the upcoming launch of the *Swift* GRB mission and *SIRTF*. These new facilities will possibly bring GRB host galaxies into the forefront of star formation studies.

*Subject headings:* cosmology: observations — galaxies: starburst — gamma rays: bursts

### 1. INTRODUCTION

One of the major thrusts in modern cosmology is an accurate census of star formation and star-forming galaxies in the universe. This endeavor forms the backbone for a slew of methods (observational, analytical, and numerical) to study the process of galaxy formation and evolution over cosmic time. To date, star-forming galaxies have been selected and studied mainly in two observational windows: the rest-frame ultraviolet (UV), and rest-frame radio and far-infrared (FIR). For galaxies at high redshift these bands are shifted into the optical and radio/submillimeter, allowing observations from the ground. Still, the problem of translating the observed emission to star formation rate (SFR) involves great uncertainty. This is partly because each band traces only a minor portion of the total energy output of stars. Moreover, the optical/UV band is significantly affected by dust obscuration, thus requiring order-of-

magnitude corrections, while the submillimeter and radio bands lack sensitivity and therefore uncover only the most prodigiously star-forming galaxies.

The main result that has emerged from star formation surveys over the past few years is exemplified in the so-called Madau diagram. Namely, the SFR volume density,  $\rho_{\text{SFR}}(z)$ , rises steeply to  $z \sim 1$  (Lilly et al. 1996) and seemingly peaks at  $z \sim 1-2$ . There is still some debate about how steep the rise is, with values ranging from  $(1+z)^{1.5}$  (Wilson et al. 2002) to  $(1+z)^4$  (e.g., Madau et al. 1996). The evolution beyond  $z \sim 2$  is even less clear since optical/UV observations indicate a decline (Madau et al. 1996), while recent submillimeter observations argue for a flat  $\rho_{\text{SFR}}(z)$  to higher redshift,  $z \sim 4$  (Barger, Cowie, & Richards 2000). Consistency with this trend can be obtained by invoking large dust corrections in the optical/UV (Steidel et al. 1999). For general reviews of star formation surveys we refer the reader to Kennicutt (1998), Adelberger & Steidel (2000), and Blain et al. (2002).

Despite the significant progress in this field, our current understanding of star formation and its redshift evolution is still limited by the biases and shortcomings of current optical/UV, submillimeter, and radio selection techniques. In particular, despite the fact that the optical/UV band is sensitive to galaxies with modest SFRs (down to a fraction of a  $M_{\odot} \text{ yr}^{-1}$ ) at high redshift, these surveys may miss the most dusty and vigorously star-forming galaxies. Moreover, it is

<sup>1</sup> Division of Physics, Mathematics, and Astronomy, 105-24, California Institute of Technology, Pasadena, CA 91125.

<sup>2</sup> Institute for Astronomy, University of Hawaii, 2680 Woodlawn Drive, Honolulu, HI 96822.

<sup>3</sup> National Radio Astronomy Observatory, Socorro, NM 87801.

<sup>4</sup> Department of Astronomy, University of Wisconsin, 475 North Charter Street, Madison, WI 53706.

<sup>5</sup> Department of Physics and Astronomy, University of Hawaii, 2505 Correa Road, Honolulu, HI 96822.

not clear if the simple, locally calibrated, prescriptions for correcting the observed “unobscured” SFR for dust extinction (e.g., Meurer, Heckman, & Calzetti 1999), hold at high redshift; even if they do, these prescriptions involve an order-of-magnitude correction above and beyond the inherent uncertainty in the conversion factors. Finally, the optical/UV surveys are magnitude-limited and therefore miss the faintest sources.

Submillimeter surveys have uncovered a population of highly dust-extincted galaxies, which are usually optically faint and have SFRs of several hundred  $M_{\odot} \text{ yr}^{-1}$  (e.g., Smail, Ivison, & Blain 1997). However, unlike optical/UV surveys, submillimeter surveys are severely sensitivity limited and only detect galaxies with  $L_{\text{bol}} \gtrsim 10^{12} L_{\odot}$ . More importantly, current submillimeter bolometer arrays (such as the Submillimeter Common-User Bolometer Array [SCUBA]) have large beams on the sky ( $\sim 15''$ ), making it difficult to unambiguously identify optical counterparts (which are usually faint to begin with) and hence measure the redshifts (Smail et al. 2002); in fact, of the  $\sim 200$  submillimeter galaxies identified to date, only a handful have a measured redshift. Finally, translating the observed submillimeter emission to an SFR requires significant assumptions about the temperature of the dust and the dust emission spectrum (e.g., Blain et al. 2002).

Surveys at decimeter radio wavelengths also suffer from low sensitivity, but the high astrometric accuracy afforded by synthesis arrays such as the Very Large Array (VLA)<sup>6</sup> allows a subarcsecond localization of the radio-selected galaxies. As a result, it is easier to identify the optical counterparts of these sources. Recently, this approach has been used to preselect sources for targeted submillimeter observations resulting in an increase in the submillimeter detection rate (Barger et al. 2000; Chapman et al. 2002a) and redshift determination (Chapman et al. 2003). However, this method is biased toward finding luminous (high SFR) sources since it requires an initial radio detection. An additional problem with radio, even more than with submillimeter, selection is contamination by active galactic nuclei (AGNs). An examination of the X-ray properties of radio- and submillimeter-selected galaxies reveals that on the order of 20% can have a significant AGN component (Barger et al. 2001).

The most significant problem with current star formation studies, however, is that the link between the optical and submillimeter/radio samples is still not well understood. The Hubble Deep Field (HDF) provides a clear illustration: the brightest submillimeter source does not appear to have an optical counterpart (Hughes et al. 1998), and only recently has a detection been claimed in the near-IR (NIR;  $K \approx 23.5$  mag; Dunlop et al. 2002). Along the same line, submillimeter observations of the optically selected Lyman break galaxies have resulted in very few detections (Chapman et al. 2000, 2002b; Peacock et al. 2000), and even the brightest Lyman break galaxies appear to be faint in the submillimeter band (Baker et al. 2001). In addition, there is considerable diversity in the properties of optical counterparts to submillimeter sources, ranging from galaxies that are faint in both the optical and NIR to those that are bright in both bands (Ivison et al. 2000; Smail et al. 2002).

As a result of the unclear overlap, and the sensitivity and dust problems in the submillimeter and optical surveys, there is still strong disagreement about the fractions of global star formation in the optical and submillimeter/radio-selected galaxies (e.g., Adelberger & Steidel 2000; Scott et al. 2002). It is therefore not clear if the majority of star formation takes place in ultraluminous galaxies with very high SFRs, or in the more abundant lower luminosity galaxies with SFRs of a few  $M_{\odot} \text{ yr}^{-1}$ . Given the difficulty with redshift identification of submillimeter galaxies, the redshift distribution of dusty star-forming galaxies remains highly uncertain.

One way to alleviate some of these problems is to study a sample of galaxies that is immune to the selection biases of current optical/UV and submillimeter/radio surveys and that may draw a more representative sample of the underlying distribution of star-forming galaxies. The host galaxies of gamma-ray bursts (GRBs) may provide one such sample.

The main advantages of the sample of GRB host galaxies are as follows:

1. The galaxies are selected with no regard to their emission properties in any wavelength regime.
2. The dust-penetrating power of the gamma-ray emission results in a sample that is completely unbiased with respect to the global dust properties of the hosts.
3. GRBs can be observed to very high redshifts with existing missions ( $z \gtrsim 10$ ; Lamb & Reichart 2000), and as a result volume corrections for the SFRs inferred from their hosts are trivial.
4. The redshift of the galaxy can be determined via absorption spectroscopy of the optical afterglow or X-ray spectroscopy, allowing a redshift measurement of arbitrarily faint galaxies (the current record-holder is the host of GRB 990510 with  $R = 28.5$  mag and  $z = 1.619$ ; Vreeswijk et al. 2001b).
5. Since there is excellent circumstantial evidence linking GRBs to massive stars (e.g., Bloom, Kulkarni, & Djorgovski 2002), the sample of GRB hosts may trace global star formation (Blain & Natarajan 2000).

Of course, the sample of GRB hosts is not immune from its own problems and potential biases. First, the sample is much smaller than the optical and submillimeter samples<sup>7</sup> (although the number of GRB hosts with a known redshift exceeds the number of submillimeter galaxies with a measured redshift). As a result, at the present, it is not possible to assess the SFR density that is implied by GRB hosts or its redshift evolution. Moreover, despite the link between GRBs and massive stars, it is not clear whether GRB progenitors are truly representative of massive stars. In particular, a bias toward subsolar metallicity for GRB progenitors (and hence their environments) has been discussed (MacFadyen & Woosley 1999; MacFadyen, Woosley, & Heger 2001), but it appears that very massive stars (e.g.,  $M \gtrsim 35 M_{\odot}$ ) should produce black holes even at solar metallicity. The impact of metallicity on additional aspects of GRB formation (e.g., angular momentum, loss of hydrogen envelope) is not clear at present.

Regardless of the exact details of these potential biases and problems, it is safe to conclude that GRB hosts provide

<sup>6</sup> The VLA is operated by the National Radio Astronomy Observatory, a facility of the National Science Foundation operated under cooperative agreement by Associated Universities, Inc.

<sup>7</sup> Currently, the sample of GRB hosts numbers about 30 sources, and grows at a rate of about one per month. The upcoming *Swift* mission is expected to increase the rate to one per 2–3 days.

a new perspective of global star formation, which is at least subject to a different set of systematic problems than the optical/UV and submillimeter approach.

To date, GRB host galaxies have mainly been studied in the optical and NIR bands. With the exception of one source (GRB 020124; Berger et al. 2002), every GRB localized to a subarcsecond position has been associated with a star-forming galaxy (Bloom et al. 2002). These galaxies range from  $R \approx 22$  to 29 mag, have a median redshift  $\langle z \rangle \sim 1$ , and are generally typical of star-forming galaxies at similar redshifts in terms of morphology and luminosity (Djorgovski et al. 2001b), with SFRs from optical spectroscopy of  $\sim 1\text{--}10 M_{\odot} \text{ yr}^{-1}$ . At the same time, there are hints for higher than average ratios of  $[\text{Ne III}] \lambda 3869$  to  $[\text{O II}] \lambda 3727$ , possibly indicating the presence of massive stars (Djorgovski et al. 2001b). Only two host galaxies have been detected so far in the radio (GRB 980703; Berger, Kulkarni & Frail 2001) and submillimeter (GRB 010222; Frail et al. 2002).

Here we present submillimeter and radio observations of a sample of 20 GRB host galaxies, ranging in redshift from about 0.4 to 4.5 (§ 2); one of the 20 sources is detected with high significance in both the submillimeter and radio bands, and an additional source is detected in the submillimeter (§ 3). We compare the detected submillimeter and radio host galaxies to local and high- $z$  ultraluminous galaxies in § 4 and derive the SFRs in § 5. We then compare the inferred SFRs of the detected host galaxies, and the ensemble of undetected hosts, to optical estimates in § 6. Finally, we compare the optical properties of the GRB host galaxies to those of submillimeter- and radio-selected star-forming galaxies (§ 7).

## 2. OBSERVATIONS

### 2.1. Target Selection

At the time we conducted our survey, the sample of GRB host galaxies numbered 25, of which 20 had measured redshifts. These host galaxies were localized primarily based on optical afterglows but also using the radio and X-ray afterglow emission. Of the 25 host galaxies, we observed eight in both the radio and submillimeter, seven in the radio, and five in the submillimeter. The galaxies were drawn from the list of 25 hosts at random, constrained primarily by the availability of observing time. Thus, the sample presented here does not suffer from any obvious selection biases, with the exception of detectable afterglow emission in at least one band.

Submillimeter observations of GRB afterglows and a small number of host galaxies have been undertaken in the past. Starting in 1997, Smith et al. (1999, 2001) have searched for submillimeter emission from the afterglow of thirteen GRBs. While they did not detect any afterglow emission, these authors used their observations to place constraints on emission from eight host galaxies, with typical  $1 \sigma$  rms values of 1.2 mJy. Since these were target-of-opportunity observations, they were not always undertaken in favorable observing conditions.

More recently, Barnard et al. (2002) reported targeted submillimeter observations of the host galaxies of four optically dark GRBs (i.e., GRBs lacking an optical afterglow). They focused on these particular sources because one explanation for the lack of optical emission is obscuration

by dust, which presumably points to a dusty host. None of the hosts were detected, with the possible exception of GRB 000210 (see § 3.4), leading the authors to conclude that the hosts of dark bursts are not necessarily heavily dust-obscured.

Thus, the observations presented here provide the most comprehensive and bias-free search for submillimeter emission from GRB host galaxies, and the first comprehensive search for radio emission.

### 2.2. Submillimeter Observations

Observations in the submillimeter band were carried out using SCUBA (Holland et al. 1999) on board the James Clerk Maxwell Telescope (JCMT).<sup>8</sup> We observed the positions of 13 well-localized GRB afterglows with the long (850  $\mu\text{m}$ ) and short (450  $\mu\text{m}$ ) arrays. The observations, summarized in Table 1, were conducted in photometry mode with the standard nine-jiggle pattern using the central bolometer in each of the two arrays to observe the source. In the case of GRB 000301C, we used an off-center bolometer in each array because of high noise levels in the central bolometer.

To account for variations in the sky brightness, we used a standard chopping of the secondary mirror between the on-source position and a position 60'' away in azimuth, at a frequency of 7.8125 Hz. In addition, we used a two-position beam switch (nodding), in which the beam is moved off-source in each exposure to measure the sky. Measurements of the sky opacity (sky dips) were taken approximately every 2 hr, and the focus and array noise were checked at least twice during each shift.

The pointing was checked approximately once per hour using several sources throughout each shift and was generally found to vary by  $\lesssim 3''$  (i.e., less than one-quarter of the beam size). All observations were performed in band 2 and 3 weather with  $\tau_{225\text{GHz}} \approx 0.05\text{--}0.12$ .

The data were initially reduced with the SCUBA Data Reduction Facility (SURF) following the standard reduction procedure. The off-position pointings were subtracted from the on-position pointings to account for chopping and nodding of the telescope. Noisy bolometers were removed to facilitate a more accurate sky subtraction (see below), and the data were then flat-fielded to account for the small differences in bolometer response. Extinction correction was performed using a linear interpolation between sky dips taken before and after each set of on-source scans.

In addition to the sky subtraction offered by the nodding and chopping, short-term sky contributions were subtracted by using all low-noise off-source bolometers (sky bolometers). This procedure takes advantage of the fact that the sky contribution is correlated across the array. As a result, the flux in the sky bolometers can be used to assess the sky contribution to the flux in the on-source bolometer. This procedure is especially crucial when observing weak sources, since the measured flux may be dominated by the sky. We implemented the sky subtraction using SURF and our own routine using MATLAB. We found that, in general, the SURF sky subtraction underestimated the sky contribution and, as a result, overestimated the source

<sup>8</sup> The JCMT is operated by the Joint Astronomy Centre on behalf of the Particle Physics and Astronomy Research Council of the UK, the Netherlands Organization for Scientific Research, and National Research Council of Canada.



TABLE 1  
SUBMILLIMETER OBSERVATIONS

Source (1)	$z$ (2)	Observation Date (UT) (3)	$F_\nu(350 \text{ GHz})$ (mJy) (4)	$F_\nu(670 \text{ GHz})$ (mJy) (5)	$\langle F_\nu(350 \text{ GHz}) \rangle$ (mJy) (6)
GRB 970228 .....	0.695	2001 Nov 1	$-1.58 \pm 1.34$	$-21.4 \pm 18.6$	
		2001 Nov 2	$0.42 \pm 1.61$	$-10.9 \pm 21.4$	$-0.76 \pm 1.03$
GRB 970508 .....	0.835	2001 Sep 9	$-1.70 \pm 1.56$	$-12.2 \pm 48.4$	
		2001 Sep 10	$-0.53 \pm 1.60$	$3.2 \pm 64.8$	
		2001 Sep 12	$-3.64 \pm 2.43$	$6.0 \pm 34.2$	$-1.57 \pm 1.01$
GRB 971214 .....	3.418	2001 Nov 2	$0.49 \pm 1.11$	$-14.2 \pm 12.6$	$0.49 \pm 1.11$
GRB 980329 .....	...	2001 Sep 13	$1.22 \pm 1.62$	$8.6 \pm 10.2$	
		2001 Oct 29	$2.06 \pm 0.99$	$-27.4 \pm 21.6$	$1.83 \pm 0.84$
GRB 980613 .....	1.096	2001 Nov 1	$2.84 \pm 1.87$	$92.6 \pm 95.9$	
		2001 Nov 2	$2.21 \pm 1.77$	$30.3 \pm 64.4$	
		2001 Dec 7	$0.93 \pm 1.33$	$22.6 \pm 17.6$	$1.75 \pm 0.92$
GRB 980703 .....	0.966	2001 Sep 10	$-2.40 \pm 1.30$	$-22.6 \pm 18.6$	
		2001 Sep 12	$-0.84 \pm 1.33$	$-13.9 \pm 10.7$	$-1.64 \pm 0.93$
GRB 991208 .....	0.706	2001 Dec 6	$-2.65 \pm 1.83$	$9.1 \pm 26.9$	
		2001 Dec 7	$-0.08 \pm 1.42$	$26.0 \pm 17.2$	$-1.04 \pm 1.12$
GRB 991216 .....	1.020	2001 Oct 31	$0.09 \pm 1.20$	$-6.5 \pm 21.3$	
		2001 Nov 3	$1.23 \pm 1.85$	$-30.2 \pm 31.1$	
		2001 Nov 4	$0.73 \pm 2.60$	$25.6 \pm 128.5$	$0.47 \pm 0.94$
GRB 000210 .....	0.846	2001 Sep 12	$3.96 \pm 2.27$	$98.1 \pm 48.2$	
		2001 Sep 13	$4.34 \pm 1.63$	$70.1 \pm 45.1$	
		2001 Sep 14	$-0.01 \pm 1.87$	$-6.4 \pm 87.1$	$2.97 \pm 0.88$
GRB 000301C.....	2.034	2001 Dec 29	$1.02 \pm 1.99$	$21.4 \pm 10.7$	
		2001 Dec 30	$-2.71 \pm 1.79$	$-18.7 \pm 25.1$	$-1.04 \pm 1.33$
GRB 000418 .....	1.119	2001 Oct 30	$3.80 \pm 2.11$	$9.4 \pm 56.7$	
		2001 Oct 31	$3.59 \pm 1.35$	$65.1 \pm 31.4$	
		2001 Nov 1	$2.32 \pm 1.46$	$31.9 \pm 26.1$	$3.15 \pm 0.90$
GRB 000911 .....	1.058	2001 Sep 13	$0.56 \pm 1.69$	$4.7 \pm 22.7$	
		2001 Sep 14	$-0.37 \pm 2.68$	$-11.1 \pm 41.2$	
		2001 Oct 31	$0.95 \pm 2.25$	$-35.0 \pm 66.2$	
		2001 Nov 3	$6.73 \pm 2.08$	$56.5 \pm 52.3$	
		2001 Nov 4	$3.07 \pm 1.82$	$-49.0 \pm 51.3$	$2.31 \pm 0.91$
GRB 011211 .....	2.140	2001 Dec 29	$1.64 \pm 1.61$	$8.1 \pm 15.2$	
		2001 Dec 30	$-0.11 \pm 1.60$	$-14.3 \pm 42.7$	
		2001 Dec 31	$3.88 \pm 2.26$	$17.7 \pm 68.0$	$1.39 \pm 1.01$

NOTE.—Col. (1): Source name; col. (2): source redshift; col. (3): UT date for each observation; col. (4): flux density at 350 GHz; col. (5): flux density at 670 GHz; col. (6): weighted-average flux density at 350 GHz.

fluxes; the discrepancy in fluxes varied from about 0.1 to 0.5 mJy. Since the discrepancies were not severe, and to maintain a conservative approach, we used the results of our own analysis routine. For this purpose we calculated the median value of the two (three) outer rings of bolometers in the 850  $\mu\text{m}$  (450  $\mu\text{m}$ ) array, after removing noisy bolometers (defined as those whose standard deviation over a whole scan deviated by more than  $5\sigma$  from the median standard deviation of all sky bolometers).

Following the sky subtraction, we calculated the mean and standard deviation of the mean (SDOM) for each source in a given observing shift. Noisy data were eliminated in two ways. First, the data were binned into 25 equal time bins, and the SDOM was calculated step-wise, i.e., at each step the data from an additional bin were added and the mean and SDOM were recalculated. In an ideal situation where the data quality remains approximately constant, the SDOM should progressively decrease as more data are accumulated. However, if the quality of the data worsens (due to deteriorating weather conditions for example) the SDOM will increase. We therefore removed time bins in which the SDOM increased. After applying this procedure, we recursively eliminated individual noisy data

points using a  $\sigma$  cutoff level based on the number of data points (Chauvenet's criterion; Taylor 1982) until the mean converged on a constant value. Typically, two or three iterations were required, with only a few data points rejected each time. For all sources only a few percent of the data were rejected by the two procedures.

Finally, flux conversion factors (FCFs) were applied to the resulting voltage measurements to convert the signal to janskys. Using photometry observations of Mars and Uranus, and/or secondary calibrators (OH 231.8+4.2, IRC+10216, and CRL 618), we found the FCF to vary between 180 and 205 Jy  $\text{V}^{-1}$  at 850  $\mu\text{m}$ , consistent with the typical value of  $197 \pm 13$ . At 450  $\mu\text{m}$ , the FCFs varied between 250 and 450 Jy  $\text{V}^{-1}$ .

### 2.3. Radio Observations

*Very Large Array.*—We observed 12 GRB afterglow positions with the VLA from 2001 April to 2002 February. All sources were observed at 8.46 GHz in the standard continuum mode with  $2 \times 50$  MHz bands. In addition, GRB 000418 was observed at 1.43 and 4.86 GHz, and GRB 0010222 was observed at 4.86 GHz. In Table 2 we provide a summary of the observations.

TABLE 2  
RADIO OBSERVATIONS

Source (1)	$z$ (2)	Telescope (3)	Observation Dates (UT) (4)	Observation Frequency (GHz) (5)	$F_\nu$ ( $\mu$ Jy) (6)
GRB 970828 .....	0.958	VLA	2001 Jun 4–7	8.46	$12 \pm 9$
GRB 980329 .....	...	VLA	2001 Jul 22–Sep 10	8.46	$18 \pm 8$
GRB 980613 .....	1.096	VLA	2001 May 18–26	8.46	$11 \pm 12$
GRB 981226 .....	...	VLA	2001 Jul 24–Oct 15	8.46	$21 \pm 12$
GRB 991208 .....	0.706	VLA	2001 Apr 14–Jul 20	8.46	$21 \pm 9$
GRB 991216 .....	1.020	VLA	2001 Jun 8–Jul 13	8.46	$11 \pm 9$
GRB 000210 .....	0.846	VLA	2001 Sep 16–Oct 12	8.46	$18 \pm 9$
GRB 000301C.....	2.034	VLA	2001 Jun 15–Jul 22	8.46	$23 \pm 7$
GRB 000418 .....	1.119	VLA	2002 Jan 14–Feb 27	1.43	$69 \pm 15$
		VLA	2001 Dec 8–2002 Jan 10	4.86	$46 \pm 13$
		VLA	2001 May 28–Jun 3	8.46	$51 \pm 12$
GRB 000911 .....	1.058	VLA	2001 Mar 21–Apr 2	8.46	$6 \pm 17$
GRB 000926 .....	2.037	VLA	2001 Jun 11–Jul 12	8.46	$33 \pm 9$
GRB 010222 .....	1.477	VLA	2001 Sep 29–Oct 13	4.86	$19 \pm 10$
		VLA	2001 Jun 24–Aug 27	8.46	$17 \pm 6$
GRB 990510 .....	1.619	ATCA	2002 Apr 28	1.39	$9 \pm 35$
GRB 990705 .....	0.840	ATCA	2002 Apr 21–22	1.39	$40 \pm 34$
GRB 000131 .....	4.5	ATCA	2002 Apr 28	1.39	$52 \pm 32$
GRB 000210 .....	0.846	ATCA	2002 Apr 27–28	1.39	$80 \pm 52$

NOTE.—Col. (1): Source name; col. (2): source redshift; col. (3): telescope; col. (4): range of UT dates for each observation; col. (5): observing frequency; col. (6): peak flux density at the position of each source.

In principle, since the median spectrum of faint radio sources between 1.4 and 8.5 GHz is  $F_\nu \propto \nu^{-0.6}$  (Fomalont et al. 2002), the ideal VLA frequency for our observations (taking into account the sensitivity at each frequency) is 1.43 GHz. However, we chose to observe primarily at 8.46 GHz for the following reason. The majority of our observations were taken in the BnC, C, CnD, and D configurations, in which the typical synthesized beam size is  $\sim 10''$ – $40''$  at 1.43 GHz, compared to  $\sim 2''$ – $8''$  at 8.46 GHz. The large synthesized beam at 1.43 GHz, combined with the larger field of view and higher intrinsic brightness of radio sources at this frequency, would result in a significant decrease in sensitivity due to source confusion. Thus, we were forced to observe at higher frequencies, in which the reduced confusion noise more than compensates for the typical steep spectrum. We chose 8.46 GHz rather than 4.86 GHz since the combination of 20% higher sensitivity and 60% lower confusion noise provide a more significant impact than the typical 30% decrease in intrinsic brightness. The 1.43 GHz observations of GRB 000418 were undertaken in the A configuration, where confusion does not play a limiting role.

For flux calibration we used the extragalactic sources 3C 48 (J0137+331), 3C 147 (J0542+498), and 3C 286 (J1331+305), while the phases were monitored using calibrator sources within  $\sim 5^\circ$  of the survey sources.

We used the Astronomical Image Processing System (AIPS) for data reduction and analysis. For each source we co-added all the observations prior to producing an image to increase the final signal-to-noise ratio (S/N).

*Australia Telescope Compact Array (ATCA).*<sup>9</sup>—We observed the positions of four GRB afterglows during 2002 April, in the 6A configuration at 1344 and 1432 MHz. Using the 6 km baseline resulted in a significant decrease in confu-

sion noise, thus allowing observations at the most advantageous frequencies. The observations are summarized in Table 2.

We used J1934–638 for flux calibration, while the phase was monitored using calibrator sources within  $\sim 5^\circ$  of the survey sources. The data were reduced and analyzed using the Multichannel Image Reconstruction, Image Analysis, and Display (MIRIAD) package and AIPS.

#### 2.4. Optical Data

The photometric and spectroscopic optical/NIR data used in this paper (see §§ 6 and 7) have been collected from the literature. Host galaxy optical and NIR magnitudes are given in the Vega magnitude system. In addition, the SFRs obtained from various optical estimators are corrected for extinction within the host galaxy when an estimate of the extinction is available (e.g., using the Balmer decrement; Djorgovski et al. 1998).

### 3. RESULTS

The flux measurements at the position of each GRB are given in Tables 1 and 2 and are plotted in Figure 1. Of the 20 sources, only GRB 000418 was detected in both the radio and submillimeter with  $S/N > 3$  (§ 3.1). One additional source, GRB 000210, is detected with  $S/N > 3$  when combining our observations with those of Barnard et al. (2002). Two hosts have radio fluxes with  $3 < S/N < 4$  (GRB 000301C and GRB 000926), but as we show below this is due in part to emission from the afterglow.

The typical  $2\sigma$  thresholds are about 2 mJy, 20  $\mu$ Jy, and 70  $\mu$ Jy in the SCUBA, VLA, and ATCA observations, respectively. In Figure 1 we plot all sources with  $S/N > 3$  as detections, and the rest as  $2\sigma$  upper limits. In addition, for the sources observed with ATCA, we plot both the 1.4 GHz upper limits and the inferred upper limits at 8.46 GHz

<sup>9</sup> The Australia Telescope is funded by the Commonwealth of Australia for operations as a National Facility managed by CSIRO.

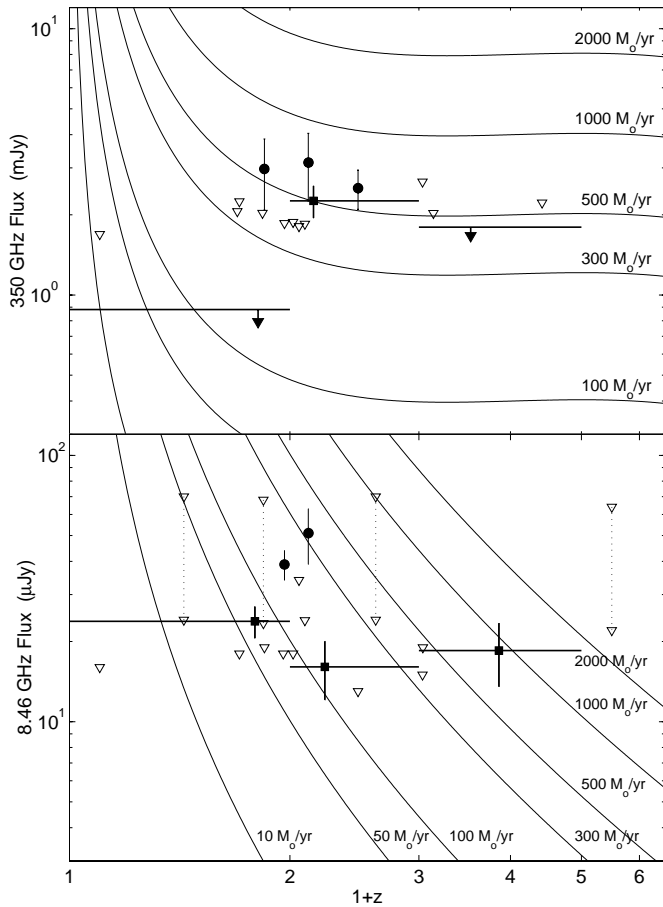


FIG. 1.—Submillimeter (*top*) and radio (*bottom*) fluxes for 20 GRB host galaxies plotted as a function of source redshift. The solid symbols are detections ( $S/N > 2$  in the submillimeter and  $S/N > 3$  in the radio), while the inverted triangles are  $2\sigma$  upper limits. In the bottom panel, the upper limits linked by dotted lines are the upper limits from the ATCA observations at 1.4 GHz (*upper triangles*) converted to 8.46 GHz (*lower triangles*) using  $F_\nu \propto \nu^{-0.6}$ . Also plotted are the ATCA upper limit for GRB 990712 ( $z = 0.433$ ; Vreeswijk et al. 2001a), the VLA detection of the host of GRB 980703 (Berger et al. 2001), and the submillimeter detection of the host of GRB 010222 (Frail et al. 2002). The source at  $1+z = 1.2$  in both panels is the host of GRB 980329, which does not have a measured redshift. The points and upper limits with horizontal error bars are weighted average fluxes in the redshift bins:  $0 < z < 1$ ,  $1 < z < 2$ , and  $z > 2$ . Finally, the thin lines are contours of constant SFR (using eq. [1] with the parameters specified in § 5).

assuming a typical radio spectrum,  $F_\nu \propto \nu^{-0.6}$  (Fomalont et al. 2002).

One obvious source for the observed radio and submillimeter fluxes (other than the putative host galaxies) is emission from the afterglows. To assess the possibility that our observations are contaminated by flux from the afterglows, we note that the observations have been undertaken at least a year after the GRB explosion.<sup>10</sup> On this timescale, the submillimeter emission from the afterglow is expected to be much lower than the detection threshold of our observations. In fact, the brightest submillimeter afterglows to date have only reached a flux of a few mJy (at 350 GHz) and typically exhibited a fading rate of  $\sim t^{-1}$  after about 1 day following the burst (Smith et al. 1999, 2001; Berger et al. 2000; Frail et al. 2002; Yost et al. 2002). Thus, on the

timescale of our observations, the expected submillimeter flux from the afterglows is only  $\sim 10 \mu\text{Jy}$ , well below the detection threshold.

The radio emission from GRB afterglows is more long-lived and hence possess a more serious problem. However, on the typical timescale of the radio observations, the 8.46 GHz flux is expected to be at most a few  $\mu\text{Jy}$  (e.g., Berger et al. 2000).

In the following sections we discuss the individual detections in the radio and submillimeter and also provide an estimate for the radio emission from each afterglow.

### 3.1. GRB 000418

A source at the position of GRB 000418 is detected at four of the five observing frequencies with  $S/N > 3$ . The SCUBA source, which we designate SMM 12252+2006, has a flux density of  $F_\nu(350 \text{ GHz}) \approx 3.2 \pm 0.9 \text{ mJy}$  and  $F_\nu(670 \text{ GHz}) \approx 41 \pm 19 \text{ mJy}$ . These values imply a spectral index,  $\beta \approx 3.9^{+1.1}_{-1.3}$  ( $F_\nu \propto \nu^\beta$ ), consistent with a thermal dust spectrum as expected if the emission is due to obscured star formation.

The radio source (VLA 122519.26+200611.1) is located at  $\alpha(\text{J2000}) = 12^{\text{h}}25^{\text{m}}19^{\text{s}}.255$ ,  $\delta(\text{J2000}) = 20^\circ06'11''.10$ , with an uncertainty of  $0''.1$  in both coordinates. This position is offset from the position of the radio afterglow of GRB 000418 (Berger et al. 2001) by  $\Delta\alpha = -0''.40 \pm 0''.14$  and  $\Delta\delta = -0''.04 \pm 0''.17$  (Fig. 2). In comparison, the offset measured from Keck and *Hubble Space Telescope* (HST) images is smaller,  $\Delta\alpha = -0''.019 \pm 0''.066$  and  $\Delta\delta = 0''.012 \pm 0''.058$ .

VLA 122519.26+200611.1 has an observed spectral slope  $\beta = -0.17 \pm 0.25$ , flatter than the typical value for faint radio galaxies,  $\beta \approx -0.6$  (Fomalont et al. 2002), and similar to the value measured for the host of GRB 980703,

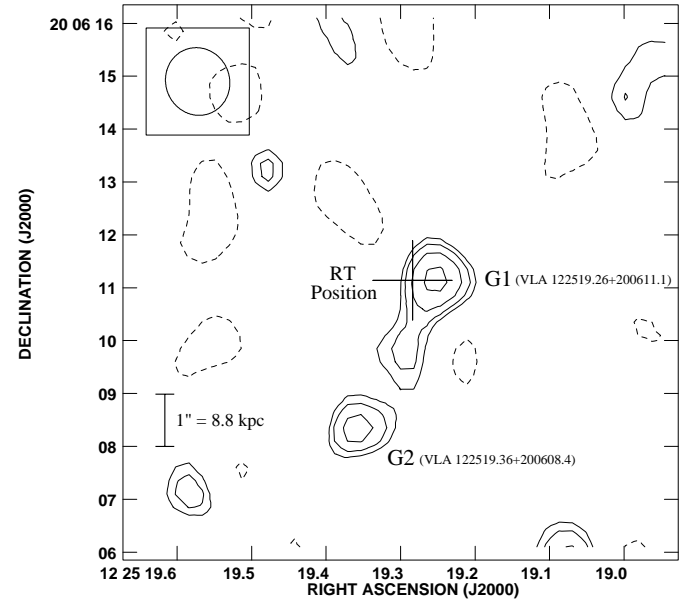


FIG. 2.—Contour plot of a  $5 \times 5 \text{ arcsec}^2$  field observed at 1.43 GHz and centered on the position (Berger et al. 2001) of the radio transient associated with GRB 000418 (*plus sign*). Contours are plotted at  $-2^{1/2}$ ,  $2^{1/2}$ ,  $2^1$ ,  $2^{3/2}$ ,  $2^2$ , and  $2^{5/2}$ . Source G1 is the host galaxy of GRB 000418, while source G2 is a possible companion galaxy. In addition, there appears to be a bridge of radio emission connecting galaxies G1 and G2. A comparison to the synthesized beam (*upper left corner*) reveals that G1 and G2 are slightly extended.

<sup>10</sup> The single exception is GRB 011211 for which SCUBA observations were taken 18–20 days after the burst.



$\beta \approx -0.32$  (Berger et al. 2001). The source appears to be slightly extended at 1.43 and 8.46 GHz, with a size of about  $1''$  (8.8 kpc at  $z = 1.119$ ).

The expected afterglow fluxes at 4.86 and 8.46 GHz at the time of our observations are about 5 and 10  $\mu\text{Jy}$ , respectively (Berger et al. 2001). At 1.43 GHz the afterglow contribution is expected to be about 10  $\mu\text{Jy}$  based on the 4.86 GHz flux and the afterglow spectrum  $F_\nu \propto \nu^{-0.65}$ . Thus, despite the contribution from the afterglow, the radio detections of the host galaxy are still significant at better than  $3\sigma$  level. Correcting for the afterglow contribution, we find an actual spectral slope  $\beta = -0.29 \pm 0.33$ , consistent with the median  $\beta \approx -0.6$  for 8.46 GHz radio sources with a similar flux (Fomalont et al. 2002).

As with all SCUBA detections, source confusion arising from the large beam ( $D_{\text{FWHM}} \approx 14''$  at 350 GHz and  $\approx 6''$  at 670 GHz) raises the possibility that SMM 12252+2006 is not associated with the host galaxy of GRB 000418. Fortunately, the detection of the radio source, which is located  $0''.4 \pm 0''.1$  away from the position of the radio afterglow of GRB 000418, indicates that SMM 12252+2006 and VLA 122519.26+200611.1 are in fact the same source—the host galaxy of GRB 000418.

Besides the positional coincidence of the VLA and SCUBA sources, we gain further confidence of the association based on the spectral index between the two bands,  $\beta_{1.4}^{350}$ . This spectral index is redshift-dependent as a result of the different spectral slopes in the two regimes (Carilli & Yun 2000; Barger et al. 2000). We find  $\beta_{1.4}^{350} \approx 0.73 \pm 0.10$ , in good agreement with the Carilli & Yun (2000) value of  $\beta_{1.4}^{350} = 0.59 \pm 0.16$  (for the redshift of GRB 000418,  $z = 1.119$ ).

We also detect another source, slightly extended ( $\theta \approx 1''$ ), approximately  $1''.4$  east and  $2''.7$  south of the host of GRB 000418 (designated VLA 122519.36+200608.4), with  $F_\nu(1.43 \text{ GHz}) = 48 \pm 15 \mu\text{Jy}$  and  $F_\nu(8.46 \text{ GHz}) = 37 \pm 12 \mu\text{Jy}$  (see Fig. 2). This source appears to be linked by a bridge of radio emission (with S/N  $\approx 1.5$  at both frequencies) to the host of GRB 000418. The physical separation between the two sources, assuming both are at the same redshift,  $z = 1.119$ , is 25 kpc. There is no obvious optical counterpart to this source in *HST* images down to about  $R \sim 27.5$  mag.

Based purely on radio source counts at 8.46 GHz (Fomalont et al. 2002), the expected number of sources with  $F_\nu(8.46 \text{ GHz}) \approx 37 \mu\text{Jy}$  in a  $3''$  radius circle is only about  $2.7 \times 10^{-4}$ . Thus, the coincidence of two such faint sources within  $3''$  is highly suggestive of an interacting system, rather than chance superposition.

Interacting radio galaxies with separations of about 20 kpc and joined by a bridge of radio continuum emission have been observed locally (Condon et al. 1993; Condon, Helou, & Jarrett 2002). In addition, optical surveys (e.g., Patton et al. 2002) show that a few percent of galaxies with an absolute *B*-band magnitude similar to that of the host of GRB 000418, have companions within about 30 kpc. The fraction of interacting systems is possibly much higher,  $\sim 50\%$ , in ultraluminous systems (such as the host of GRB 000418), both locally (Sanders & Mirabel 1996) and at high redshift (e.g., Ivison et al. 2000).

We note that with a separation of only  $3''$ , the host of GRB 000418 and the companion galaxy fall within the SCUBA beam. Thus, it is possible that SMM 12252+2006 is, in fact, a superposition of both radio sources. This will change the value of  $\beta_{1.4}^{350}$  to about 0.46.

### 3.2. GRB 980703

The host galaxy of GRB 980703 has been detected in deep radio observations at 1.43, 4.86, and 8.46 GHz (Berger et al. 2001). The galaxy has a flux  $F_\nu(1.43 \text{ GHz}) = 68.0 \pm 6.6 \mu\text{Jy}$ , and a radio spectral slope  $\beta = -0.32 \pm 0.12$ . In addition, the radio emission is unresolved with a maximum angular size of  $0''.27$  (2.3 kpc).

Based on the Carilli & Yun (2000) value of  $\beta_{1.4}^{350} \approx 0.54 \pm 0.16$  (for the redshift of GRB 980703,  $z = 0.966$ ), the expected flux at 350 GHz is  $F_\nu(350 \text{ GHz}) \approx 1.3^{+1.9}_{-0.8} \text{ mJy}$ . The observed ( $2\sigma$ ) flux limit  $F_\nu(350 \text{ GHz}) < 1.8 \text{ mJy}$  is consistent with the expected value.

### 3.3. GRB 010222

GRB 010222 has been detected in SCUBA and IRAM observations with a persistent flux of about 3.5 mJy at 350 GHz and 1 mJy at 250 GHz (Frail et al. 2002). The persistent emission, as well as the steep spectral slope,  $\beta \approx 3.8$ , indicated that while the detected emission was partially due to the afterglow of GRB 010222, it was dominated by the host galaxy. In fact, accounting for the expected afterglow emission, we find that the host galaxy has a flux,  $F_\nu(350 \text{ GHz}) \approx 2.5 \pm 0.4 \text{ mJy}$ .

The radio flux predicted from the submillimeter emission (Carilli & Yun 2000) is  $F_\nu(1.43 \text{ GHz}) \approx 55^{+80}_{-20} \mu\text{Jy}$  (for  $z = 1.477$ , the redshift of GRB 010222), which corresponds to  $F_\nu(4.86 \text{ GHz}) \approx 15\text{--}60 \mu\text{Jy}$ , and  $F_\nu(8.46 \text{ GHz}) \approx 10\text{--}45 \mu\text{Jy}$  (assuming  $\beta = -0.6$ ). Therefore, our measured values,  $F_\nu(4.86 \text{ GHz}) = 26 \pm 8 \mu\text{Jy}$  and  $F_\nu(8.46 \text{ GHz}) = 17 \pm 6 \mu\text{Jy}$  are consistent with the observed submillimeter emission.

The expected afterglow fluxes at 4.86 and 8.46 GHz are 3 and 4  $\mu\text{Jy}$ , respectively, significantly lower than the measured values. Thus, the observed flux mainly arises from the host.

### 3.4. GRB 000210

Recently, Barnard et al. (2002) measured a flux of  $3.3 \pm 1.5 \text{ mJy}$  for GRB 000210, in good agreement with our value of  $2.8 \pm 1.1 \text{ mJy}$ . A weighted average (here and elsewhere we use inverse-variance weighting) of the two measurements gives  $F_\nu(350 \text{ GHz}) = 3.0 \pm 0.9 \text{ mJy}$ , similar to the submillimeter flux from the host galaxies of GRB 000418 and GRB 010222. The radio flux at the position of GRB 000210 is  $F_\nu(8.46 \text{ GHz}) = 18 \pm 9 \mu\text{Jy}$ . Based on a redshift of 0.846 (Piro et al. 2002) and the submillimeter detection, the expected radio flux from this source (Carilli & Yun 2000) is  $F_\nu(8.46 \text{ GHz}) \approx 10\text{--}50 \mu\text{Jy}$ , consistent with the measured value. The expected flux of the afterglow at the time of the radio observations is less than 1  $\mu\text{Jy}$  (Piro et al. 2002).

### 3.5. GRB 980329

Following the localization of GRB 980329, Smith et al. (1999) observed the afterglow position with SCUBA and claimed the detection of a source with a 350 GHz flux of about  $5.0 \pm 1.5 \text{ mJy}$  on 1998 April 5.2 UT. Subsequent observations indicated a fading trend, with a decline to  $4.0 \pm 1.2 \text{ mJy}$  on April 6.2, and less than 1.8 mJy ( $2\sigma$ ) on April 11.2. Based on a comparison to the radio flux of the afterglow, Smith et al. (1999) concluded that the detected submillimeter flux was in excess of the emission from the

afterglow itself, and therefore requires an additional component, most likely a host galaxy.

Recently, Yost et al. (2002) reanalyzed the SCUBA data and showed that the initial submillimeter flux was, in fact, only about 2.5 mJy, and perfectly consistent with the afterglow flux. As a result, it is not clear that an additional persistent component is required. We also reanalyzed the data from 1998 April using the method described in § 2.2. We find the following fluxes:  $2.4 \pm 1.0$  mJy (April 5),  $2.4 \pm 1.1$  mJy (April 6),  $1.2 \pm 0.8$  mJy (April 7),  $1.4 \pm 0.9$  mJy (April 8), and  $1.6 \pm 0.8$  mJy (April 11). A comparison to the results in Smith et al. (1999) reveals that, with the exception of the last epoch, they overestimate the fluxes by about 0.5–2.5 mJy.

Our observations of GRB 980329 from 2001 September and October reveal a flux,  $F_\nu(350 \text{ GHz}) = 1.8 \pm 0.8$  mJy, indicating that the flattening to a value of about 1.5 mJy in the late epochs of the 1998 April observations may indicate emission from the host galaxy.

The radio observations are similarly inconclusive, with  $F_\nu(8.46 \text{ GHz}) = 18 \pm 8 \mu\text{Jy}$ . We estimate that the flux of the afterglow at 8.46 GHz at the time of our observations is only 1–2  $\mu\text{Jy}$  (Yost et al. 2002). Since the redshift of GRB 980329 is not known, we cannot assess the expected ratio of the radio and submillimeter fluxes.

### 3.6. GRB 000926

This source is detected in the VLA observations with a flux of  $F_\nu(8.46 \text{ GHz}) = 33 \pm 9 \mu\text{Jy}$  ( $3.7 \sigma$ ). The expected flux from the afterglow at the time of the observations,  $\approx 420$  days after the burst, is 10  $\mu\text{Jy}$  (Harrison et al. 2001). Thus, the observed emission exceeds the afterglow flux by  $2.6 \sigma$ . In the calculations below we use a host flux of  $23 \pm 9 \mu\text{Jy}$ .

### 3.7. GRB 000301C

The VLA observations of this GRB position reveal a source with  $F_\nu(8.46 \text{ GHz}) = 23 \pm 7 \mu\text{Jy}$  ( $3.1 \sigma$ ). The flux of the afterglow at the time of the observations is about 5  $\mu\text{Jy}$  (Berger et al. 2000). Thus, the excess emission is significant at the  $2.5 \sigma$  level.

The submillimeter emission predicted based on the Carilli & Yun (2000) relation is  $F_\nu(350 \text{ GHz}) = 1.5^{+3.7}_{-1.1}$  mJy (for  $z = 2.034$ , the redshift of GRB 000301C). This value is in agreement with the measured flux of  $-1 \pm 1.3$  mJy.

## 4. SPECTRAL ENERGY DISTRIBUTIONS

In Figure 3 we plot the radio-to-UV spectral energy distributions (SEDs) of the detected host galaxies of GRB 980703, GRB 000418, and GRB 010222, as well as that of Arp 220, a prototypical local ultraluminous IR galaxy (ULIRG; Soifer et al. 1984), and ERO J164502+4626.4 (HuR 10), a high- $z$  analog of Arp 220 (Hu & Ridgway 1994; Elbaz et al. 2002). The luminosities are plotted as a function of rest-frame frequencies to facilitate a direct comparison.

The detected GRB hosts are somewhat brighter than Arp 220 ( $L \approx 2 \times 10^{12} L_\odot$ ,  $\text{SFR} \approx 300 M_\odot \text{ yr}^{-1}$ ) and are similar in luminosity to HuR 10 ( $L \approx 7 \times 10^{12} L_\odot$ ,  $\text{SFR} \sim 10^3 M_\odot \text{ yr}^{-1}$ ; Dey et al. 1999). As such, we expect the host galaxies to have SFRs of a few  $\times 100 M_\odot \text{ yr}^{-1}$  and bolometric luminosities in excess of  $10^{12} L_\odot$ .

On the other hand, the average luminosity in the submillimeter band for all the observed hosts (detected and

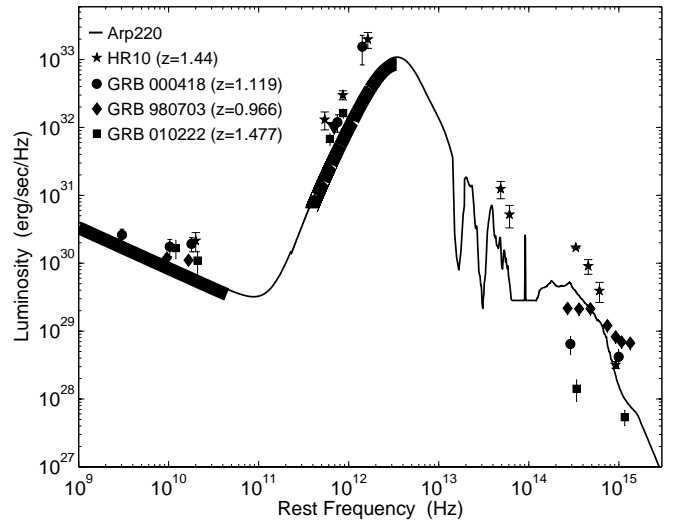


FIG. 3.—SEDs of the host galaxies of GRB 000418, GRB 980703, and GRB 010222 compared to the SED of the local starburst galaxy Arp 220, and the high- $z$  starburst galaxy HuR 10. The luminosities are plotted at the rest frequencies to facilitate a direct comparison. The GRB host galaxies are more luminous than Arp 220 and are similar to HuR 10, indicating that their bolometric luminosities exceed  $10^{12} L_\odot$ , and their SFRs are on the order of  $500 M_\odot \text{ yr}^{-1}$ . On the other hand, the spectral slopes in the optical regime are flatter than both Arp 220 and HuR 10, indicating that the GRB host galaxies are bluer than Arp 220 and HuR 10.

nondetected) is  $\langle L_{\nu,s} \rangle \approx 2.1 \times 10^{31} \text{ ergs s}^{-1} \text{ Hz}^{-1}$  at an effective rest-frame frequency of  $7.9 \times 10^{11} \text{ Hz}$ , a factor of 3 less luminous than Arp 220. Similarly, in the radio band, at an effective frequency of 18 GHz, the average luminosity,  $\langle L_{\nu,r} \rangle \approx 6.5 \times 10^{29} \text{ ergs s}^{-1} \text{ Hz}^{-1}$ , is a factor of 4 less luminous than Arp 220.

In Figure 3 we use a more sophisticated approach to study the average SED of all GRB hosts in this survey by scaling the SED of Arp 220 using a  $\chi^2$  statistic. We find that the average SED of GRB hosts is 20% fainter in both the submillimeter and radio bands than Arp 220. This clearly indicates that, on average, GRBs select galaxies that are less luminous than the typical submillimeter-selected ULIRGs and are therefore more representative of the general population of star-forming galaxies.

In the optical/NIR, the properties of the detected GRB hosts are distinctly different than those of Arp 220 and HuR 10 (as well as other local and high- $z$  ULIRGs). In particular, from Figure 3 it is clear that while the GRB host galaxies are similar to HuR 10 and Arp 220 in the radio and submillimeter bands, their optical/NIR colors (as defined for example by  $R-K$ ) are much bluer. Moreover, while there is a dispersion of a factor of a few in the radio and submillimeter bands between the GRB hosts, HuR 10, and Arp 220, the dispersion in the optical/NIR luminosity is about 2 orders of magnitude. This indicates that there is no simple correlation between the optical/NIR luminosities of GRB hosts (and possibly other galaxies; Adelberger & Steidel 2000) and their FIR and radio luminosities. In the following sections we expound on both points.

## 5. STAR FORMATION RATES

To evaluate the SFRs that are implied by the submillimeter and radio measurements, we use the following



expression for the observed flux as a function of SFR (Yun & Carilli 2002):

$$F_\nu(\nu_{\text{obs}}) = \left\{ 25f_{\text{nth}}\nu_0^{-\beta} + 0.71\nu_0^{-0.1} + 1.3 \times 10^{-6}\nu_0^3 \frac{1 - \exp[-(\nu_0/2000)^{1.35}]}{\exp(0.00083\nu_0) - 1} \right\} \times \frac{(1+z)\text{SFR}}{d_L^2} \text{ Jy}. \quad (1)$$

Here  $\nu_0 = (1+z)\nu_{\text{obs}}$  GHz, SFR is the star formation rate in  $M_\odot \text{ yr}^{-1}$ ,  $d_L$  is the luminosity distance in Mpc, and  $f_{\text{nth}}$  is a scaling factor (of order unity), which accounts for the difference in the conversion between synchrotron flux and SFR in the Milky Way and other galaxies. The first term on the right-hand side accounts for the fact that nonthermal synchrotron emission arising from supernova remnants is proportional to the SFR, while the second term is the contribution of free-free emission from H II regions. These two flux terms dominate in the radio regime.

The last term in equation (1) is the dust spectrum, which dominates in the submillimeter and FIR regimes. In this case, the parameters that have been chosen to characterize the spectrum are a dust temperature,  $T_d = 58$  K, and a dust emissivity,  $\beta = 1.35$ , based on a sample of 23 IR-selected starburst galaxies with  $L_{\text{FIR}} > 10^{11} L_\odot$  (Yun & Carilli 2002). We note that other authors (e.g., Blain et al. 2002) favor a lower dust temperature,  $T_d \approx 40$  K, which would result in SFRs that are higher by about 70%.

To calculate  $d_L$  we use the cosmological parameters  $\Omega_m = 0.3$ ,  $\Omega_\Lambda = 0.7$ , and  $H_0 = 65 \text{ km s}^{-1} \text{ Mpc}^{-1}$ . We also use the typical value  $\beta \approx -0.6$  for the radio measurements (Fomalont et al. 2002). In Figure 1 we plot contours of a constant SFR overlaid on the submillimeter and radio flux measurements. Our radio observations are sensitive to galaxies with  $\text{SFR} > 100 M_\odot \text{ yr}^{-1}$  at  $z \sim 1$ , and  $\text{SFR} > 1000 M_\odot \text{ yr}^{-1}$  at  $z \sim 3$ . The submillimeter flux, on the other hand, is relatively constant for a given SFR, independent of  $z$ . This is due to the large positive  $k$ -correction resulting from the steep thermal dust spectrum. Therefore, at the typical limit of our submillimeter observations, we are sensitive to galaxies with  $\text{SFR} \gtrsim 500 M_\odot \text{ yr}^{-1}$ .

For the host galaxies that are detected with  $\text{S/N} > 3$  in the submillimeter and radio, as well as those detected in the past (i.e., GRB 980703 and GRB 010222), we calculate the following star formation rates: GRB 000418– $\text{SFR}_S = 690 \pm 200 M_\odot \text{ yr}^{-1}$ ,  $\text{SFR}_R = 330 \pm 75 M_\odot \text{ yr}^{-1}$ ; GRB 000210– $\text{SFR}_S = 560 \pm 170 M_\odot \text{ yr}^{-1}$ ; GRB 010222– $\text{SFR}_S = 610 \pm 100 M_\odot$ ; GRB 980703– $\text{SFR}_R = 180 \pm 25 M_\odot \text{ yr}^{-1}$ . Here  $\text{SFR}_S$  and  $\text{SFR}_R$  are the SFRs derived from the submillimeter and radio fluxes, respectively. We note that the difference in the radio and submillimeter derived SFRs for GRB 000418 are an indication of the uncertainty in the dust properties and the parameter  $f_{\text{nth}}$ .

The detections and upper limits from this survey, combined with the detections and upper limits discussed in the literature (Berger et al. 2001; Vreeswijk et al. 2001a; Frail et al. 2002) indicate that about 20% of all GRBs explode in galaxies with SFRs of a few  $\times 100 M_\odot \text{ yr}^{-1}$ . A similar conclusion has been reached from the shape of the 850  $\mu\text{m}$  background (Barger, Cowie, & Sanders 1999). At the same

time, it is clear that  $\sim 80\%$  of GRB host galaxies have more modest star formation rates,  $\text{SFR} \lesssim 100 M_\odot \text{ yr}^{-1}$ .

Despite the fact that the majority of the survey sources are not detected, we can ask the question of whether the GRB host galaxies exhibit a significant submillimeter and/or radio emission *on average*. The weighted average emission from the nondetected sources ( $\text{S/N} < 3$ ) is  $\langle F_\nu(350 \text{ GHz}) \rangle = 0.37 \pm 0.34 \text{ mJy}$ , and  $\langle F_\nu(8.46 \text{ GHz}) \rangle = 17.1 \pm 2.7 \mu\text{Jy}$ . This average radio flux is possibly contaminated by flux from the afterglows at the level of about  $3 \mu\text{Jy}$ , so we use  $\langle F_\nu(8.46 \text{ GHz}) \rangle \approx 14 \pm 2.7 \mu\text{Jy}$  ( $5.2 \sigma$ ). Therefore, as an ensemble, the GRB host galaxies exhibit radio emission but no significant submillimeter emission. Using the median redshift,  $z \approx 1$ , for the nondetected sample, the average radio flux implies an average  $\langle \text{SFR}_R \rangle \approx 100 M_\odot \text{ yr}^{-1}$ , while the submillimeter  $2 \sigma$  upper limit on  $\langle \text{SFR}_S \rangle$  is about  $150 M_\odot \text{ yr}^{-1}$ .

The average submillimeter flux can be compared to  $\langle F_\nu(350 \text{ GHz}) \rangle = 0.8 \pm 0.3 \text{ mJy}$  for the nondetected submillimeter sources in a sample of radio-preselected, optically faint ( $I > 25 \text{ mag}$ ) galaxies (Chapman et al. 2001),  $\langle F_\nu(350 \text{ GHz}) \rangle = 0.4 \pm 0.2 \text{ mJy}$  for Lyman break galaxies (Webb et al. 2003), or  $\langle F_\nu(350 \text{ GHz}) \rangle \approx 0.2 \text{ mJy}$  for optically selected starbursts in the HDF (Peacock et al. 2000). Thus, it appears that GRB host galaxies trace a somewhat fainter population of submillimeter galaxies compared to the radio-preselected sample, but similar to the Lyman break and HDF samples. This is not surprising given that the radio preselection is naturally biased in favor of luminous sources.

We can further extend this analysis by calculating the average submillimeter and radio fluxes in several redshift bins. Here we include both detections and upper limits. From the submillimeter (radio) observations we find  $\langle F_\nu \rangle = -0.2 \pm 0.4 \text{ mJy}$  ( $\langle F_\nu \rangle = 24 \pm 3 \mu\text{Jy}$ ) for  $z = 0-1$ ,  $\langle F_\nu \rangle = 2.3 \pm 0.3 \text{ mJy}$  ( $\langle F_\nu \rangle = 16 \pm 4 \mu\text{Jy}$ ) for  $z = 1-2$ , and  $\langle F_\nu \rangle = 0.5 \pm 0.7 \text{ mJy}$  ( $\langle F_\nu \rangle = 18 \pm 5 \mu\text{Jy}$ ) for  $z > 2$ . These average fluxes are marked in Figure 1. In the submillimeter there is a clear increase in the average flux from  $z < 1$  to  $z \sim 1-2$ , and a flattening or decrease beyond  $z \sim 2$ . In the radio, on the other hand, the average flux is about the same in all three redshift bins.

The average radio fluxes translate into the following star formation rates for  $z < 1$  the inferred average SFR is  $\sim 110 M_\odot \text{ yr}^{-1}$ , for  $1 < z < 2$  it is  $\sim 200 M_\odot \text{ yr}^{-1}$ , and for  $z > 2$  it is  $\sim 700 M_\odot \text{ yr}^{-1}$  (with  $> 3 \sigma$  significance in each bin). The submillimeter observations on the other hand, indicate a rise from a value of  $\lesssim 160 M_\odot \text{ yr}^{-1}$  for  $z < 1$  to  $\sim 510 M_\odot \text{ yr}^{-1}$  for  $1 < z < 2$ , followed by a decline to  $\lesssim 320 M_\odot \text{ yr}^{-1}$  for  $z > 2$ . The difference between the two sets of SFR estimates is probably a combination of the stronger redshift dependence in the radio band and the inherent uncertainties in the conversion factors (e.g., dust properties).

## 6. COMPARISON TO OPTICAL OBSERVATIONS

The typical unobscured SFRs inferred from optical spectroscopy (i.e., using the UV continuum, recombination lines, and forbidden lines) are on the order of  $1-10 M_\odot \text{ yr}^{-1}$  (e.g., Djorgovski et al. 2001b). In particular, the host galaxy of GRB 980703 has an optical SFR of about  $10 M_\odot \text{ yr}^{-1}$  (Djorgovski et al. 1998), compared to about  $180 M_\odot \text{ yr}^{-1}$  from the radio observations. Similarly, the host of GRB 000418 has an optical SFR of about  $55 M_\odot \text{ yr}^{-1}$  (Bloom et

al. 2002), compared to about  $300\text{--}700 M_{\odot} \text{ yr}^{-1}$  based on the radio and submillimeter detections, while the host of GRB 000210 has an optical SFR of  $\sim 3 M_{\odot} \text{ yr}^{-1}$  compared to about  $550 M_{\odot} \text{ yr}^{-1}$  from the submillimeter observations. Finally, the average radio SFR for the nondetected sources,  $\sim 100 M_{\odot} \text{ yr}^{-1}$ , significantly exceeds the average optical SFR. This information is summarized in Figure 4 and Table 3.

The discrepancy between the optical and radio/submillimeter SFRs indicates that the majority of the star formation in the GRB host galaxies that are detected in the submillimeter and radio is obscured by dust. It is possible that the same is true for the sample as a whole, but this relies on the less-secure average SFR in the non-detected hosts. The significant dust obscuration is not surprising given that a similar trend has been noted in high- $z$  starburst galaxies, for which the typical dust corrections (based on the UV slope technique) are an order of magnitude (Meurer et al. 1999). In this case we find similar correction factors.

We can also assess the level of obscuration by comparing the UV luminosity at  $1600 \text{ \AA}$ ,  $L_{1600}$ , to the bolometric dust luminosity,  $L_{\text{bol, dust}}$ . The ratio of these two quantities provides a rough measure of the obscuration, while the sum provides a rough measure of the total SFR (Adelberger & Steidel 2000). To estimate  $L_{1600}$  we use the following host magnitudes:  $B \approx 23.2$  mag (GRB 980703; Bloom et al. 1998),  $U \approx 23.5$  mag (GRB 000210; Gorosabel et al. 2002),  $R \approx 23.6$  mag (GRB 000418; Berger et al. 2001), and  $B \approx 26.7$  mag (GRB 010222; Frail et al. 2002). We extrapolate to rest-frame  $1600 \text{ \AA}$  using the mean value of  $\langle U-R \rangle \approx 0.8$  mag found for Balmer-break galaxies, and

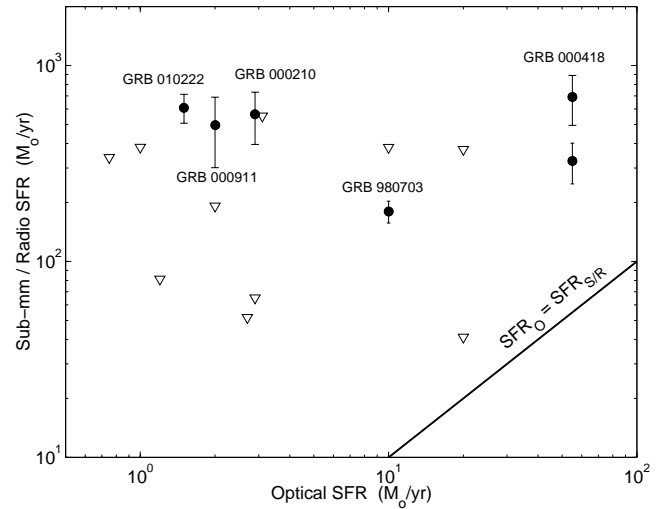


FIG. 4.—Submillimeter/radio vs. optical (i.e., from luminosity of UV continuum, recombination lines, and forbidden lines) SFRs for several GRB host galaxies. The line in the bottom right corner designates a one-to-one correspondence between the two SFRs. Clearly, the hosts that gave appreciable submillimeter and/or radio flux have a large fraction of obscured star formation. In fact, the GRB hosts with a higher dust bolometric luminosity have a higher fraction of obscured star formation.

$\langle U-R \rangle \approx 1.6$  mag found for  $z \sim 1$  galaxies in the HDF that have the largest values of  $L_{\text{bol, dust}}$ . These colors correspond to spectral slopes of  $-2.4$  and  $-3.8$ , respectively. The resulting values of  $L_{1600}$  are  $(3.4\text{--}5.2) \times 10^{10} L_{\odot}$  (GRB 980703),  $(3.1\text{--}4.0) \times 10^{10} L_{\odot}$  (GRB 000210),  $(0.8\text{--}1.8) \times 10^{10} L_{\odot}$  (GRB 000418), and  $(0.9\text{--}1.0) \times 10^{10} L_{\odot}$  (GRB 010222); the

TABLE 3  
DERIVED STAR FORMATION RATES

Source (1)	Submillimeter SFR ( $M_{\odot} \text{ yr}^{-1}$ ) (2)	Radio SFR ( $M_{\odot} \text{ yr}^{-1}$ ) (3)	Optical SFR ( $M_{\odot} \text{ yr}^{-1}$ ) (4)
GRB 970228 .....	<335	...	1
GRB 970508 .....	<380	...	1
GRB 970828 .....	...	$80 \pm 60$	1.2
GRB 971214 .....	$120 \pm 275$	...	3
GRB 980329 <sup>a</sup> .....	$460 \pm 210$	$615 \pm 275$	...
GRB 980613 .....	$380 \pm 200$	$50 \pm 140$	...
GRB 980703 .....	<380	$180 \pm 25$	10
GRB 981226 <sup>a</sup> .....	...	$150 \pm 85$	...
GRB 990510 .....	...	$190 \pm 750$	...
GRB 990705 .....	...	$190 \pm 165$	...
GRB 991208 .....	<370	$70 \pm 30$	20
GRB 991216 .....	<395	$80 \pm 70$	...
GRB 000131 .....	...	$9800 \pm 6070$	...
GRB 000210 .....	$560 \pm 165$	$90 \pm 45$	3
GRB 000301C .....	<670	$640 \pm 270$	...
GRB 000418 .....	$690 \pm 195$	$330 \pm 75$	55
GRB 000911 .....	$495 \pm 195$	$85 \pm 70$	2
GRB 000926 .....	...	$820 \pm 340$	...
GRB 010222 .....	$610 \pm 100$	$300 \pm 115$	1.5
GRB 011211 .....	$350 \pm 255$	...	...

NOTES.—Col. (1): Source name; col. (2): SFR derived from the submillimeter flux; col. (3): SFR derived from the radio flux; col. (4): SFR derived from various optical estimators. The upper limits represent  $2 \sigma$  values in the case when the measured flux was negative (see Table 1).

<sup>a</sup> We assume  $z = 1$ .

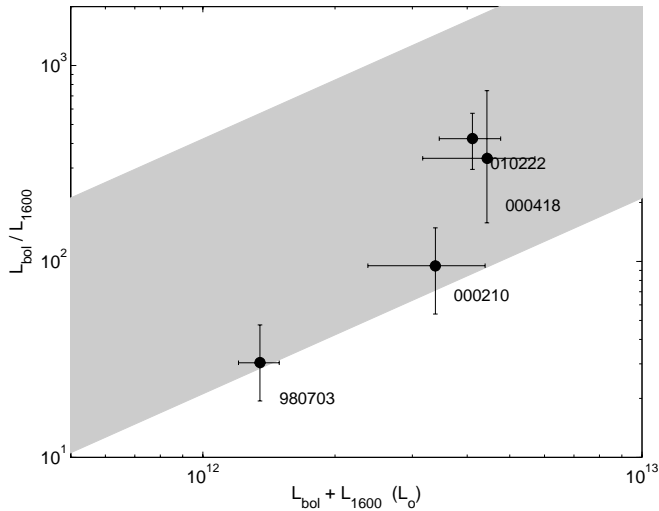


FIG. 5.—Ratio of bolometric luminosity,  $L_{\text{bol}}$  to luminosity at  $1600 \text{ \AA}$ ,  $L_{1600}$  plotted as a function of the combined luminosity. The ordinate provides a measure of the amount of dust obscuration, while the abscissa provides a measure of the total SFR. Filled circles are the host galaxies detected here and by Berger et al. (2001) and Frail et al. (2002), while the shaded region is from Adelberger & Steidel (2000) based on observations of starbursts and ULIRGs at  $z \sim 1$ . Clearly, there is a trend in both samples for more dust obscuration at higher SFRs.

lower values are for  $\beta = -3.8$ . The mean values of  $L_{1600}$ , with the uncertainty defined as a combination of the range of reasonable spectral slopes and the intrinsic uncertainty in the host magnitudes are plotted in Figure 5.

We estimate  $L_{\text{bol,dust}}$  from the submillimeter fluxes (with the exception of GRB 980703 for which we use the radio flux) using the conversion factors given in equations (2) and (5) of Adelberger & Steidel (2000). The resulting values are  $1.3 \times 10^{12} L_{\odot}$  (GRB 980703),  $3.3 \times 10^{12} L_{\odot}$  (GRB 000210),  $4.4 \times 10^{12} L_{\odot}$  (GRB 000418), and  $4.1 \times 10^{12} L_{\odot}$  (GRB 010222). Thus,  $L_{\text{bol,dust}}/L_{1600}$  evaluates to 25–40 (GRB 980703), 80–105 (GRB 000210), 245–550 (GRB 000418), and 410–455 (GRB 010222). These results, as well as the sample of starbursts and ULIRGs at  $z \sim 1$  taken from Adelberger & Steidel (2000), are plotted in Figure 4. We note that the GRB hosts are within the scatter of the  $z \sim 1$  sample, following the general trend of increasing value of  $L_{\text{bol,dust}}/L_{1600}$  (i.e., increasing obscuration) with increasing  $L_{\text{bol,dust}} + L_{1600}$  (i.e., increasing SFR).

At the same time, the particular lines of sight to the GRBs within the submillimeter/radio-bright host galaxies do not appear to be heavily obscured. For example, an extinction of  $A_V^{\text{host}} \sim 1$  mag has been inferred for GRB 980703 (Frail et al. 2003),  $A_V^{\text{host}} \sim 0.4$  mag has been found for GRB 000418 (Berger et al. 2001), and  $A_V^{\text{host}} \sim 0.1$  mag has been found for GRB 010222. The optically dark GRB 000210 suffered more significant extinction,  $A_R^{\text{host}} > 1.6$  mag. In addition, the small offset of GRB 980703 relative to its radio host galaxy ( $0''.04$ ; 0.3 kpc at the redshift of the burst), combined with the negligible extinction, indicates that while the burst probably exploded in a region of intense star formation, it either managed to destroy a large amount of dust in its vicinity or the dust distribution is patchy. It is beyond the scope of this paper to evaluate the potential of dust destruction by GRBs (see, e.g., Waxman & Draine 2000), but it is clear that the GRBs that exploded in the detected

submillimeter and radio host galaxies did not occur in the most heavily obscured star formation sites.

## 7. COMPARISON OF THE OPTICAL/NIR COLORS OF GRB HOSTS TO RADIO- AND SUBMILLIMETER-SELECTED GALAXIES

As we noted in § 4, the optical/NIR colors of the detected GRB host galaxies are bluer than those of Arp 220 ( $R-K \approx 4$  mag) and HuR 10 ( $I-J \approx 5.8$  mag; Dey et al. 1999). In this section we compare the  $R-K$  color of GRB hosts to the  $R-K$  colors of radio-preselected submillimeter galaxies (Chapman et al. 2003; Lewis et al. 2003) and submillimeter-selected galaxies with a known optical counterpart and a redshift (Frayer et al. 1998; Ivison et al. 1998; Frayer et al. 1999).

In Figure 6 we plot  $R-K$  color versus redshift for GRB hosts and radio-preselected submillimeter galaxies. The optical and NIR data are collected from the literature and are given in Vega magnitudes. Before comparing the two populations, we note that the mean  $R-K$  color and redshift for the entire GRB sample are  $2.6 \pm 0.6$  mag and  $1.0 \pm 0.3$ , respectively, and for the hosts that are detected in the submillimeter and radio they are  $2.6 \pm 0.3$  mag and  $1.1 \pm 0.3$ , respectively. Thus, there is no clear correlation between the optical/NIR colors of the GRB hosts and their submillimeter/radio luminosity.

For the sample of radio-preselected and submillimeter-selected galaxies, the mean  $R-K$  color and redshift are  $4.6 \pm 1.0$  mag and  $1.8 \pm 0.7$ , respectively. To facilitate a more direct comparison with the GRB sample we also calculate the mean values for the same redshift range as the GRB hosts:  $\langle R-K \rangle = 5.1 \pm 0.9$  mag and  $\langle z \rangle = 1.1 \pm 0.3$ . Clearly, the GRB host galaxies are, on average, significantly

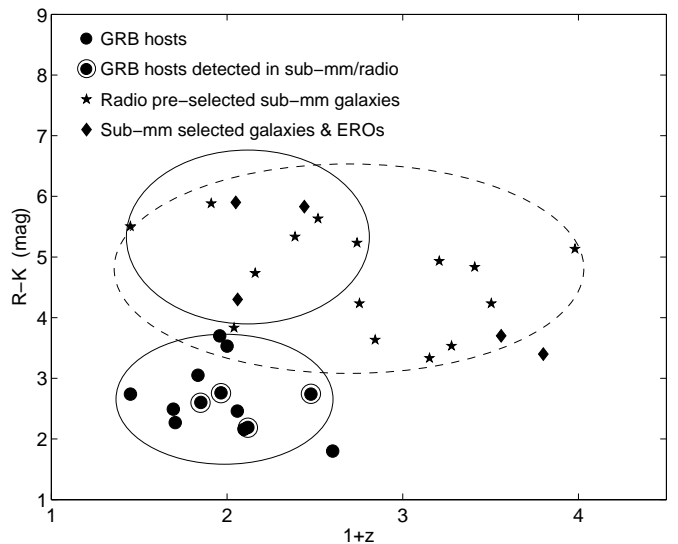


FIG. 6.— $R-K$  color as a function of redshift for GRB host galaxies and radio-preselected submillimeter-selected galaxies (Chapman et al. 2003). The solid ellipses are centered on the mean color and redshift for each population of galaxies in the redshift range  $z < 1.6$  and have widths of  $2\sigma$ . The dashed ellipse is the same for the submillimeter population as a whole. Clearly, the GRB hosts are significantly bluer than the submillimeter galaxies in the same redshift range, indicating a possible preference for younger star formation episodes in GRB selected galaxies.



bluer than galaxies selected in the radio and submillimeter in the same redshift range.

Moreover, if we examine only the host galaxies that were detected in the radio and submillimeter with high significance, we find  $R-K$  colors of 2.2 mag (GRB 000418), 2.8 mag (GRB 980703), 2.1 mag (GRB 010222), and 2.6 mag (GRB 000210). The bluest submillimeter- and radio-selected galaxies, on the other hand, have  $R-K \approx 3.1$  mag.

The obvious difference in  $R-K$  color indicates that the GRB and radio/submillimeter selections result in a somewhat different set of galaxies. The red colors of the submillimeter-selected galaxies are not surprising since these sources are expected to be dust-obscured. On the other hand, the mean color of the GRB hosts is bluer by about 2.5 mag ( $2.3 \sigma$  significance) compared to submillimeter galaxies in the same redshift range, indicating a bias toward less dust obscuration, a more patchy dust distribution, or intrinsically bluer colors.

It is possible that there is a bias toward less dust obscuration in the general GRB host sample because the bursts that explode in dusty galaxies would have obscured optical afterglows and hence no accurate localization. However, this is not a likely explanation since the GRBs that exploded in the submillimeter- and radio-bright hosts are not significantly dust-obscured (§ 6). Moreover, it does not appear that the hosts of dark GRBs are brighter in the submillimeter as expected if the dust obscuration is global (Barnard et al. 2002). Finally, the localization of afterglows in the radio and X-rays allows the selection of host galaxies even if they are dusty. In particular, the only two GRBs in which significant obscuration of the optical afterglow has been inferred (GRB 970828: Djorgovski et al. 2001a; GRB 000210: Piro et al. 2002) have been localized thanks to accurate positions from the radio and X-ray afterglows and have host galaxies with  $R-K$  colors of 3.7 and 2.6 mag, not significantly redder than the general population of GRB hosts. Therefore, a bias against dust-obscured host galaxies is not the reason for the bluer color of the sample.

An alternative explanation is that the distribution of dust in GRB hosts is different than in the radio-preselected and submillimeter-selected galaxies. This may be in terms of a spatially patchy distribution, which will allow more of the UV light to escape, or a different distribution of grain sizes (i.e., a different extinction law), possibly due to a different average metallicity. However, in both cases, it is not clear why there should be a correlation between the dust properties of the galaxy and the occurrence of a GRB.

Finally, it is possible that GRB host galaxies are preferentially in an earlier stage of the star formation (or starburst) process. In this case, a larger fraction of the shorter-lived massive stars would still be shining, and the overall color of the galaxy would be bluer relative to a galaxy with an older population of stars. One way to examine the age of the stellar population is to fit population synthesis models to the broadband optical/NIR spectra of the host galaxies. This approach has recently been used by Chary, Becklin, & Armus (2002), who find some evidence that the age of the stellar population in some GRB host galaxies (including the host of GRB 980703) is relatively young, on the order of 10–50 Myr.

This result is also expected if GRBs arise from massive stars, as indicated by recent observations (e.g., Bloom et al. 2002), since in this case GRBs would preferentially select galaxies with younger star formation episodes.

Regardless of the exact reason for the preferential selection of bluer galaxies relative to the radio-preselected submillimeter population, two results seem clear: (1) the GRB host galaxies detected in the submillimeter and radio are likely drawn from a population that is generally missed in current submillimeter surveys, and (2) GRB host galaxies may not be a completely bias-free sample.

The first point is particularly interesting in light of the fact that optical estimates of the SFR based on recombination and forbidden line luminosities do not identify them as particularly exceptional. Therefore, while similar galaxies are not necessarily missed in optical surveys, their SFRs are likely underestimated.

## 8. CONCLUSIONS AND FUTURE PROSPECTS

We presented the most comprehensive SCUBA, VLA, and ATCA observations of GRB host galaxies to date. The host galaxy of GRB 000418 is the only source detected with high significance in both the submillimeter and radio, while the host galaxy of GRB 000210 is detected with  $S/N \approx 3.3$  in the submillimeter when we combine our observations with those of Barnard et al. (2002). When taken in conjunction with the previous detections of GRB 980703 in the radio (Berger et al. 2001) and GRB 010222 in the submillimeter (Frail et al. 2002), these observations point to a  $\sim 20\%$  detection rate in the radio/submillimeter. This detection rate confirms predictions for the number of submillimeter-bright GRB hosts, with  $F_\nu(350 \text{ GHz}) \sim 3 \text{ mJy}$ , based on current models of the star formation history assuming a large fraction of obscured star formation (Ramirez-Ruiz, Trentham, & Blain 2002).

The host galaxies detected in the submillimeter and radio have SFRs from about 200 to 700  $M_\odot \text{ yr}^{-1}$ , while statistically the nondetected sources have an *average* SFR of about 100  $M_\odot \text{ yr}^{-1}$ . These SFRs exceed the values inferred from various optical estimates by over an order of magnitude, pointing to significant dust obscuration within the GRB host galaxies detected in the submillimeter and radio, and possibly the sample as a whole.

Still, the optical afterglows of the bursts that exploded in the submillimeter/radio-bright host galaxies did not suffer significant extinction, indicating that (1) the GRBs did not explode in regions where dust obscuration is significant, or (2) the UV and X-ray emission from the afterglow destroys a significant amount of dust in the local vicinity of the burst.

We have also shown that GRB host galaxies, even those detected in the submillimeter/radio, have bluer  $R-K$  colors compared to galaxies selected in the submillimeter or radio bands in the same redshift range. This is not the result of an observational bias against dusty galaxies in the GRB host sample since the afterglows of GRBs that exploded in the radio/submillimeter-bright hosts were not significantly obscured. More likely, this is the result of younger stellar populations in these galaxies or possibly a patchy dust distribution. If the reason is younger stellar population, then this provides additional circumstantial evidence in favor of massive (and hence short-lived) stars as the likely progenitors of GRBs.

A potential bias of the GRB host galaxy sample is that the popular “collapsar” model of GRBs calls for high-mass, low-metallicity stellar progenitors (MacFadyen & Woosley 1999). This may result in preferential selection of low-metallicity (and hence less dusty) host galaxies.

However, it appears that GRB progenitors can even have solar metallicity and that a very low metallicity is disfavored by the required initial conditions for a GRB explosion. Moreover, studies of the Milky Way (see Stasinska 2003 for a recent review), local galaxies (e.g., Alard 2001), and high- $z$  galaxies (e.g., Overzier et al. 2001), indicate that there are considerable variations in metallicity within galaxies. This may be especially true if several independent episodes of star formation have occurred within the galaxy. Thus, even if there is a bias toward low metallicity for GRB progenitors (and hence their immediate environments), it is not obvious that this introduces a bias in the host galaxy sample.

Nonetheless, while the observations presented in this paper clearly indicate the potential of GRB selection of high- $z$  galaxies for the study of star formation, a much larger sample is required to complement existing optical and submillimeter surveys. This may become possible in the near future with the upcoming launch (2003 September) of *Swift*. With an anticipated rapid ( $\sim 1$  minute) and accurate localization of about 150 bursts per year, the GRB-selected sample will probably increase to several hundred galaxies over the next few years. The rapid localization would most likely result in a large fraction of redshift measurements thanks to the bright optical afterglows.

In addition to the localization of a large number of GRB hosts, the study of these galaxies (as well as those in other samples) would greatly benefit from the advent of new facilities, such as *SIRTF*, ALMA, EVLA, and SKA. In Figure 7 we again plot the rest-frame SEDs of Arp 220 and the submillimeter/radio-bright GRB hosts. Overplotted on these SEDs are the  $1\sigma$  sensitivities of *SIRTF*, ALMA, and EVLA for 200 s exposures at redshifts 1 and 3, as well as the sensitivities of current instruments (VLA and SCUBA).

The contributions of these new facilities to star formation studies are threefold: (1) increased sensitivity, (2) increased resolution, and (3) increased frequency coverage. These improvements will serve to ameliorate the main limitations of present radio, submillimeter, and IR observations (§ 1) by allowing the detection of more representative star-forming galaxies at high redshift, in addition to a better constraint on the total dust bolometric luminosity and accurate localizations, which would facilitate follow-ups at optical wavelengths. In conjunction with increasingly larger samples of galaxies selected in the optical, the radio/submillimeter/IR, and by GRBs, the future of star formation studies is poised for great advances and new discoveries.

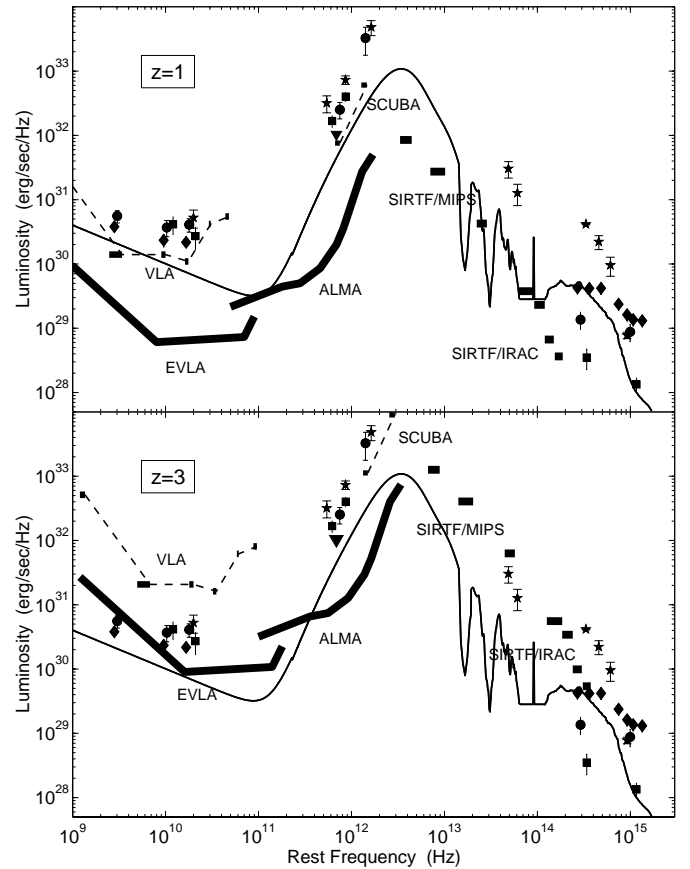


Fig. 7.—Same as Fig. 3, overplotted with the EVLA, ALMA, and *SIRTF* bands at  $z = 1$  and  $3$ . The shaded regions correspond to the  $1\sigma$  sensitivity in a 200 s exposure for each instrument, while the dashed lines are the typical  $1\sigma$  sensitivities for current instruments (i.e., VLA and SCUBA). Clearly, the new observatories will allow a significant increase in sensitivity and spectral coverage over current instruments. As a result, the radio/submillimeter/IR observations will be able to probe lower luminosity (and hence more typical) star-forming galaxies.

We thank A. Blain, A. Shapley, and the referee K. Adelberger, for helpful discussions and suggestions, and G. Moriarty-Schieven for help with the data reduction. We also thank S. Chapman for providing us with the optical/NIR colors and redshifts of radio-preselected submillimeter galaxies prior to publication.

#### REFERENCES

- Adelberger, K. L., & Steidel, C. C. 2000, *ApJ*, 544, 218  
 Alard, C. 2001, *A&A*, 377, 389  
 Baker, A. J., Lutz, D., Genzel, R., Tacconi, L. J., & Lehnert, M. D. 2001, *A&A*, 372, L37  
 Barger, A. J., Cowie, L. L., Mushotzky, R. F., & Richards, E. A. 2001, *AJ*, 121, 662  
 Barger, A. J., Cowie, L. L., & Richards, E. A. 2000, *AJ*, 119, 2092  
 Barger, A. J., Cowie, L. L., & Sanders, D. B. 1999, *ApJ*, 518, L5  
 Barnard, V., et al. 2003, *MNRAS*, 338, 1  
 Berger, E., Kulkarni, S. R., & Frail, D. A. 2001, *ApJ*, 560, 652  
 Berger, E., et al. 2000, *ApJ*, 545, 56  
 ———. 2001, *ApJ*, 556, 556  
 ———. 2002, *ApJ*, 581, 981  
 Blain, A. W., & Natarajan, P. 2000, *MNRAS*, 312, L35  
 Blain, A. W., Smail, I., Ivison, R. J., Kneib, J.-P., & Frayer, D. T. 2002, *Phys. Rep.*, 369, 111  
 Bloom, J. S., Berger, E., Kulkarni, S. R., Djorgovski, S. G., & Frail, D. A. 2002, *AJ*, submitted (astro-ph/0212123)  
 Bloom, J. S., Kulkarni, S. R., & Djorgovski, S. G. 2002, *AJ*, 123, 1111  
 Bloom, J. S., et al. 1998, *ApJ*, 508, L21  
 ———. 2002, *ApJ*, 572, L45  
 Carilli, C. L., & Yun, M. S. 2000, *ApJ*, 530, 618  
 Chapman, S. C., Lewis, G. F., Scott, D., Borys, C., & Richards, E. 2002a, *ApJ*, 570, 557  
 Chapman, S. C., Richards, E. A., Lewis, G. F., Wilson, G., & Barger, A. J. 2001, *ApJ*, 548, L147  
 Chapman, S. C., Shapley, A., Steidel, C., & Windhorst, R. 2002b, *ApJ*, 572, L1  
 Chapman, S. C., et al. 2000, *MNRAS*, 319, 318  
 ———. 2003, *ApJ*, in press  
 Chary, R., Becklin, E. E., & Armus, L. 2002, *ApJ*, 566, 229  
 Condon, J. J., Helou, G., & Jarrett, T. H. 2002, *AJ*, 123, 1881  
 Condon, J. J., Helou, G., Sanders, D. B., & Soifer, B. T. 1993, *AJ*, 105, 1730  
 Dey, A., Graham, J. R., Ivison, R. J., Smail, I., Wright, G. S., & Liu, M. C. 1999, *ApJ*, 519, 610  
 Djorgovski, S. G., Frail, D. A., Kulkarni, S. R., Bloom, J. S., Odewahn, S. C., & Diercks, A. 2001a, *ApJ*, 562, 654  
 Djorgovski, S. G., Kulkarni, S. R., Bloom, J. S., Goodrich, R., Frail, D. A., Piro, L., & Palazzi, E. 1998, *ApJ*, 508, L17  
 Djorgovski, S. G., et al. 2001b, in *Gamma-Ray Bursts in the Afterglow Era*, ed. E. Costa, F. Frontera, & J. Hjorth (Berlin: Springer), 218

- Dunlop, J., et al. 2002, MNRAS, submitted (astro-ph/0205480)
- Elbaz, D., Flores, H., Chanial, P., Mirabel, I. F., Sanders, D., Duc, P.-A., Cesarsky, C. J., & Aussel, H. 2002, A&A, 381, L1
- Fomalont, E. B., Kellermann, K. I., Partridge, R. B., Windhorst, R. A., & Richards, E. A. 2002, AJ, 123, 2402
- Frail, D. A., et al. 2002, ApJ, 565, 829
- . 2003, ApJ, submitted (astro-ph/0301421)
- Frayser, D. T., Ivison, R. J., Scoville, N. Z., Yun, M., Evans, A. S., Smail, I., Blain, A. W., & Kneib, J.-P. 1998, ApJ, 506, L7
- Frayser, D. T., et al. 1999, ApJ, 514, L13
- Gorosabel, J., et al. 2003, A&A, in press
- Harrison, F. A., et al. 2001, ApJ, 559, 123
- Holland, W. S., et al. 1999, MNRAS, 303, 659
- Hu, E. M., & Ridgway, S. E. 1994, AJ, 107, 1303
- Hughes, D. H., et al. 1998, Nature, 394, 241
- Ivison, R. J., Smail, I., Barger, A. J., Kneib, J.-P., Blain, A. W., Owen, F. N., Kerr, T. H., & Cowie, L. L. 2000, MNRAS, 315, 209
- Ivison, R. J., Smail, I., Le Borgne, J.-F., Blain, A. W., Kneib, J.-P., Bezacourt, J., Kerr, T. H., & Davies, J. K. 1998, MNRAS, 298, 583
- Kennicutt, R. C. 1998, ARA&A, 36, 189
- Lamb, D. Q., & Reichart, D. E. 2000, ApJ, 536, 1
- Lewis, G. F., Chapman, S. C., Helou, G., Borys, C., Fahlman, G., & Scott, D. 2003, ApJ, submitted
- Lilly, S. J., Le Fevre, O., Hammer, F., & Crampton, D. 1996, ApJ, 460, L1
- MacFadyen, A. I., & Woosley, S. E. 1999, ApJ, 524, 262
- MacFadyen, A. I., Woosley, S. E., & Heger, A. 2001, ApJ, 550, 410
- Madau, P., Ferguson, H. C., Dickinson, M. E., Giavalisco, M., Steidel, C. C., & Fruchter, A. S. 1996, MNRAS, 283, 1388
- Meurer, G. R., Heckman, T. M., & Calzetti, D. 1999, ApJ, 521, 64
- Overzier, R. A., Röttgering, H. J. A., Kurk, J. D., and De Breuck, C. 2001, A&A, 367, L5
- Patton, D. R., et al. 2002, ApJ, 565, 208
- Peacock, J. A., et al. 2000, MNRAS, 318, 535
- Piro, L., et al. 2002, ApJ, 577, 680
- Ramirez-Ruiz, E., Trentham, N., & Blain, A. W. 2002, MNRAS, 329, 465
- Sanders, D. B., & Mirabel, I. F. 1996, ARA&A, 34, 749
- Scott, S. E., et al. 2002, MNRAS, 331, 817
- Smail, I., Ivison, R. J., & Blain, A. W. 1997, ApJ, 490, L5
- Smail, I., Ivison, R. J., Blain, A. W., & Kneib, J.-P. 2002, MNRAS, 331, 495
- Smith, I. A., Tilanus, R. P. J., Wijers, R. A. M. J., Tanvir, N., Vreeswijk, P., Rol, E., & Kouveliotou, C. 2001, A&A, 380, 81
- Smith, I. A., et al. 1999, A&A, 347, 92
- Soifer, B. T., et al. 1984, ApJ, 283, L1
- Stasinska, G. 2003, in Cosmo chemistry: The Melting Pot of Elements, ed. C. Esteban et al. (Cambridge: Cambridge Univ. Press), in press
- Steidel, C. C., Adelberger, K. L., Giavalisco, M., Dickinson, M., & Pettini, M. 1999, ApJ, 519, 1
- Taylor, J. R. 1982, An Introduction to Error Analysis: The study of Uncertainties in Physical Measurements (Oxford: Oxford Univ. Press)
- Vreeswijk, P. M., Fender, R. P., Garrett, M. A., Tingay, S. J., Fruchter, A. S., & Kaper, L. 2001a, A&A, 380, L21
- Vreeswijk, P. M., et al. 2001b, ApJ, 546, 672
- Waxman, E., & Draine, B. T. 2000, ApJ, 537, 796
- Webb, T., et al. 2003, ApJ, 582, 6
- Wilson, G., Cowie, L. L., Barger, A. J., & Burke, D. J. 2002, AJ, 124, 1258
- Yost, S. A., et al. 2002, ApJ, 577, 155
- Yun, M. S., & Carilli, C. L. 2002, ApJ, 568, 88